Hindawi Publishing Corporation
Journal of Nanomaterials
Volume 2013, Article ID 486373, 9 pages
http://dx.doi.org/10.1155/2013/486373

Research Article

Wearout Reliability and Intermetallic Compound Diffusion Kinetics of Au and PdCu Wires Used in Nanoscale Device Packaging

C. L. Gan,[1,2] E. K. Ng,[1] B. L. Chan,[1] F. C. Classe,[3] T. Kwuanjai,[4] and U. Hashim[2]

[1] *Spansion (Penang) Sendirian Berhad, Phase II Industrial Zone, Penang, 11900 Bayan Lepas, Malaysia*
[2] *Institute of Nano Electronic Engineering (INEE), Universiti Malaysia Perlis, 01000 Kangar, Perlis, Malaysia*
[3] *Spansion Incorporation, Sunnyvale, CA 94085, USA*
[4] *Spansion (Thailand) Limited, 229 Moo 4 Changwattana Road, Nonthaburi 11120, Thailand*

Correspondence should be addressed to C. L. Gan; clgan_pgg@yahoo.com

Received 14 October 2012; Revised 15 December 2012; Accepted 16 December 2012

Academic Editor: Sheng-Rui Jian

Wearout reliability and diffusion kinetics of Au and Pd-coated Cu (PdCu) ball bonds are useful technical information for Cu wire deployment in nanoscale semiconductor device packaging. This paper discusses the HAST (with bias) and UHAST (unbiased HAST) wearout reliability performance of Au and PdCu wires used in fine pitch BGA packages. In-depth failure analysis has been carried out to identify the failure mechanism under various wearout conditions. Intermetallic compound (IMC) diffusion constants and apparent activation energies (E_{aa}) of both wire types were investigated after high temperature storage life test (HTSL). Au bonds were identified to have faster IMC formation, compared to slower IMC growth of PdCu. PdCu wire was found to exhibit equivalent or better wearout reliability margin compared to conventional Au wire bonds. Failure mechanisms of Au, Cu ball bonds post-HAST and UHAST tests are been proposed, and both Au and PdCu IMC diffusion kinetics and their characteristics are discussed in this paper.

1. Introduction

In recent years, Cu wire bonding has been widely adopted in recent nanoelectronic packaging due to its conductivity, material properties, and cost effectiveness. However, there are few key technical barriers to be seriously considered in order to achieve fully transition from Au to Cu ball bonds in semiconductor packages. Gan et al. [1–3] reported the key challenges of Cu wire bonding deployment in nanoelectronic packaging while Tan et al. [4] and Uno [5], Zhong [6], Chen et al. [7] investigated the technical barriers and engineering solutions of bare Cu and Pd-coated Cu wire bonding in semiconductor packaging. Harman [8] reported the challenges and moisture reliability of Cu wire bonding in early years. Hang et al. [9] investigated post isothermal aging of CuAl ball bonds are mainly attributed to CuAl IMC interface corrosion and induce interface microcracking. However, there are limited studies on the wearout reliability of palladium-coated Cu wire, bare Cu wire, or Au wire bonds in nanoelectronic device packaging. It is crucial to conduct knowledge-based reliability studies and understand the wearout reliability models [10] and its associated failure mechanism with Cu wire bonding in nanoelectronic device packaging which will ensure successful Cu wire bonding deployment in high pin count and nanoscale devices. McPherson [11] laid out the time to failure reliability modeling in semiconductor physics and reliability stressing. Gan et al. [12] characterized the wearout reliability on Au and Pd-coated Cu ball bonds used in fineline BGA flash memory packages. Some researchers have investigated and compared the IMC diffusion kinetics and calculated the apparent activation energy for Cu and Au ball bonds IMCs after high temperature aging [13–21] and predict E_{aa} for isothermal Cu wire interfacial fracture [22]. In the first part of this study, Au and Pd-coated Cu bonds reliability are investigated under biased HAST and UHAST; resulting wearout reliability plots are generated, and

Table 1: Characteristics of the Weibull plots of various reliability tests (Au and PdCu wires used in 110 nm device).

Wire type	Test type	Test conditions	t_{first} (hr)	t_{50}	$t_{63.2}$ (η)	β
PdCu	HAST (3.6 V Bias)	130°C, 85% RH	1817	3593	3849	5.06
Au	HAST (3.6 V Bias)	130°C, 85% RH	1553	2584	2752	4.96
PdCu	UHAST (Unbiased)	130°C, 85% RH	3000	8971	10124	3.44
Au	UHAST (Unbiased)	130°C, 85% RH	4000	9222	10189	2.82
PdCu	TC	−40°C to 150°C	7000	12544	13301	5.79
Au	TC	−40°C to 150°C	6000	11982	12922	4.72
PdCu	HTSL	150°C, 175°C, 200°C	N/A	N/A	N/A	N/A
Au	HTSL	150°C, 175°C, 200°C	N/A	N/A	N/A	N/A

Table 2: Summary of IMC diffusion kinetics and activation energies comparing Au and PdCu ball bonds used in 110 nm device packaging.

IMC Type	HTSL test conditions	E_{aa} (eV)	D_o (m^2s^{-1})	Reference
CuAl	175, 200, 250	0.63 to 0.78	1.21×10^{-7}	[13, 14]
CuAl	200, 250, 300	1.01	1.21×10^{-7}	[15]
CuAl	150, 200	1.34	1.63×10^{-4}	[16]
CuAl	Unknown	2.04	2.00×10^{-5}	[17]
CuAl	175, 200, 225, 250	1.26	3.70×10^{-5}	[18]
CuAl	150, 250, 300	1.14	N/A	[19, 20]
CuAl	**150, 175, 200**	**1.18**	$\mathbf{1.43 \times 10^{-8}}$	**This work**
AuAl	Unknown	1.80	9.10×10^{-6}	[17]
AuAl	Unknown	1.00	2.62×10^{-7}	[21]
AuAl	**150, 175, 200**	**1.04**	$\mathbf{1.97 \times 10^{-9}}$	**This work**

failure mechanisms are discussed. In the second part, HTSL aging stress is used to investigate IMC diffusion kinetics and determine the apparent activation energy (E_{aa}) for IMC growth. The values of E_{aa} and the diffusion constant D_o are then compared to values from previous studies [13–21].

2. Experimental

2.1. Materials and Preparation. The key materials used include 0.8 mil Pd-coated Cu wire and 4 N (99.99% purity) Au wire and 110 nm flash devices packaged into fortified fine-pitch BGA packages, with green (<15 ppm Chloride in content) molding compound and substrate. In this Cu wire development study, there are a total of 6 legs comprising of Pd-coated Cu wire and 4 N Au wire bonded on Fine pitch 64-ball BGA packages on a 2 L substrate. Sample size used is 80 units for each stresses. The corresponding stress tests and its conditions are tabulated in Table 1. After electrical test, good samples were then subjected for preconditioning and 3 times reflow at 260°C as described in JEDEC IPC-STD 020 standard, followed by unbiased HAST stress testing per JESD22-A118 at 130°C/85% RH [23], biased HAST stress per JESD22-A110 at 130°C/85% RH, and 3.60 V and temperature cycling per JESD22-A104 at −40°C to 150°C. Electrical testing was conducted after several readpoints of stress as well as to check Au and PdCu ball bonds integrity in terms of their moisture and thermomechanical reliability.

Another set of materials were used to characterize IMC (intermetallic compound) growth rate, diffusion kinetics, and its apparent activation energies (E_{aa}). The key materials used include 0.8 mil Pd-coated Cu wire and 4 N (99.99% purity) Au wire, fine pitch BGA package, 110 nm device that to be packed in fortified fineline BGA package, green (<20 ppm Chloride in content) in molding compound and substrate. All direct material used in this evaluation study for the 110 nm flash device (with top Al metallization bondpad) are for packaging purpose. A total of 2 legs of 45 units of Au and Pd-coated Cu wires bonded on Fine pitch 64-ball BGA packages are subjected for 150°C, 175°C, and 200°C aging temperatures. Electrical testing was conducted after each hour and cycle of stress to check Au and PdCu ball bonds integrity in terms of its high temperature ball bonds reliability with various aging conditions. IMC thickness measurements were carried out for each aging hours. D_o and apparent activation energies (E_{aa}) of AuAl and CuAl IMC diffusion kinetics were analyzed as tabulated in Table 2. The package construction of our evaluation vehicle is shown in Figure 1 with 110 nm device encapsulated with green molding compound and bonded with PdCu or Au ball bonds.

3. Results and Discussion

3.1. Wearout Reliability of Au and PdCu Ball Bonds in HAST and UHAST. Wearout reliability of Au and PdCu ball bonds were fitted to the Weibull distribution. The characteristic values of Weibull plots for both Au and PdCu ball bonds are tabulated in Table 1, covering HAST and UHAST. For HAST testing, it clearly indicates that the PdCu ball bond exhibits higher wearout reliability margins with a higher time to first failure (t_{first}) as well as a higher mean time to failure (t_{50}). In UHAST, PdCu ball bonds demonstrate a lower time to first failure compared with Au bonds the mean time to failure is similar between the two. The respective characteristic life or scale parameter ($t_{63.2}$, η), and shape

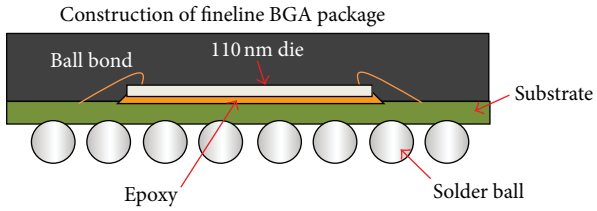

Figure 1: Package construction with 110 nm device encapsulated with Au and Cu ball bonds.

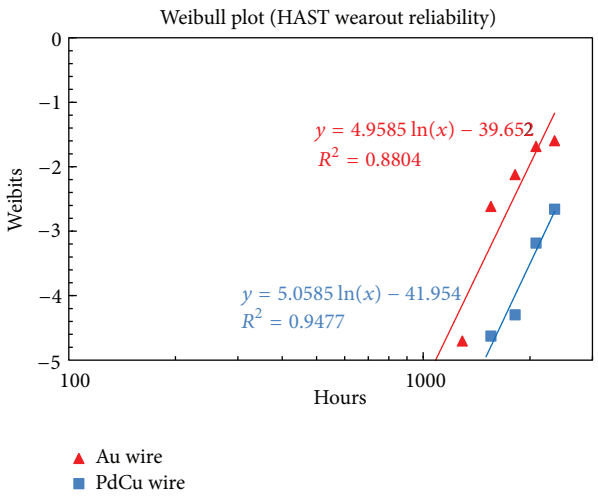

Figure 2: Biased HAST (130°C, 85% RH, 3.6 V Bias) Weibull plotting and its characteristics of PdCu and Au wires used in 110 nm device FBGA 64 package.

parameter (β) of each weibull distribution are calculated and shown in Table 1. All reliability plots belong to wear out reliability region in conventional reliability bathtub curve since the shape parameters (β) are more than 1.0 for biased HAST, UHAST, and TC stresses.

Samples loaded for temperature cycling (TC) stress (−40°C to 150°C). It also reveals higher cycles-to-failure for PdCu ball bonds compared to Au ball bonds.

3.1.1. Weibull Plots Analysis and Characterization. Cu wire is well known to be less corrosion resistant compared to Au wire in nanoelectronic packaging. Moisture reliability of bare Cu wire is identified as a key technical barrier of Cu wire deployment in nanoelectronic packaging. Cu ball bond interfacial fracture is one of the bonding failures attributed to interface CuAl IMC corrosion [1–5, 7, 8, 12, 24, 25]. Figure 2 indicates the wearout reliability Weibull plot comparing PdCu wire and Au wire. In our evaluation, the PdCu Weibull plot actually shows a higher reliability margin than Au in HAST stress. This is most likely due to that Pd-coated Cu ball bond exhibits higher moisture reliability margin as Pd in Cu ball bond is more resistant towards moisture corrosion under biased HAST conditions. In our study, we use alternative method for performing Weibull plotting through the use of Weibits. The conversion of cumulative fraction failed, F into

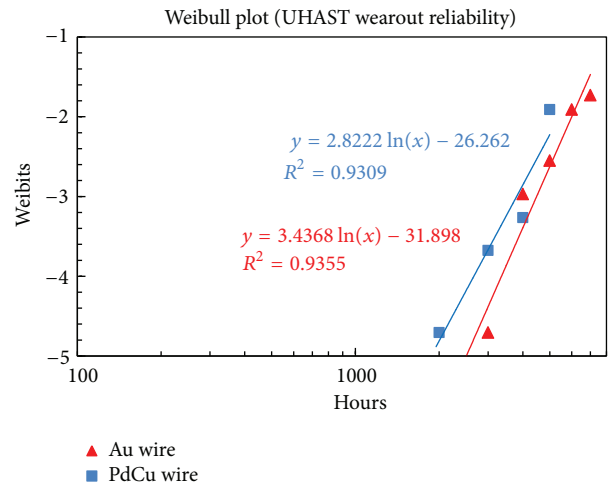

Figure 3: Unbiased HAST (85% RH, 130°C) Weibull plotting and its characteristics of PdCu and Au wires used in 110 nm device FBGA 64 package.

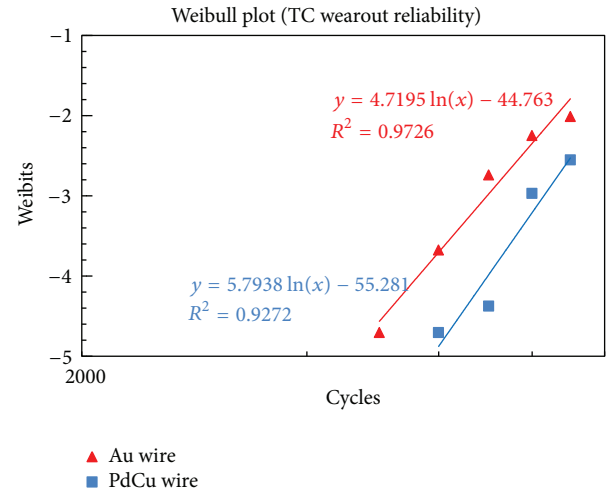

Figure 4: Component level temperature cycling (−40°C to 150°C) Weibull plotting and its characteristics of PdCu and Au wires used in 110 nm device FBGA 64 package.

Weibits, that is given by Weibits is equivalent to $\ln[-\ln(1-F)]$ [11].

However, PdCu wire exhibits slightly lower UHAST stress compared to conventional Au wire as shown in Figure 3. This could be attributed to the variation of PdCu ball bond integrity in semiconductor assembly. However, both PdCu and Au wire legs in UHAST stress still far exceeded the industrial JEDEC standard of 96-hour surviving hours. The first hour rate to failure of PdCu and Au ball bonds are at 3000 hour and 4000 hour, respectively. This indicates that the bare Cu wire coated with palladium plays an important role in improving its biased HAST wearout reliability compared to Au ball bond in FBGA package with longer surviving hours.

Thermomechanical degree of Au and PdCu ball bonds was investigated through Temperature Cycling, (−40°C to 150°C condition TC). Figure 4 reveals wearout reliability plots

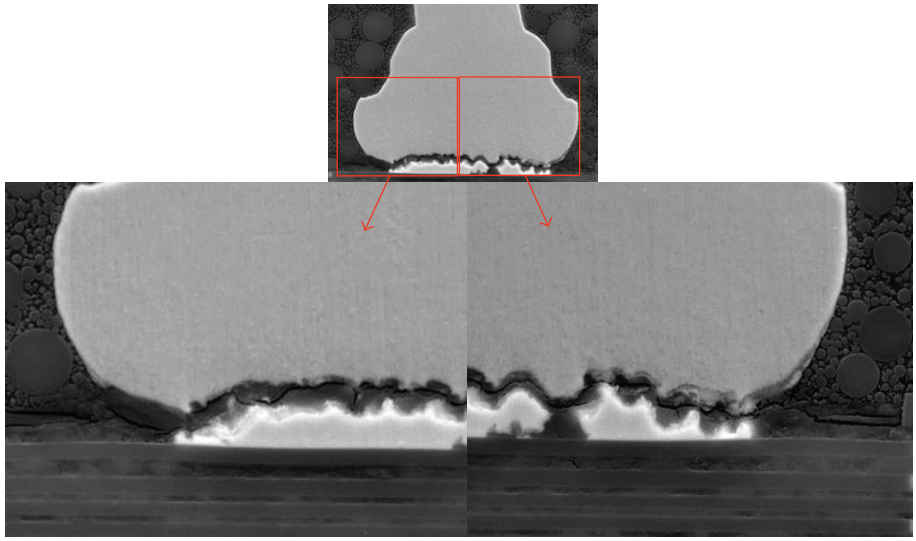

Figure 5: Typical AuAl IMC microcracks post extended HAST stress (1553 hr).

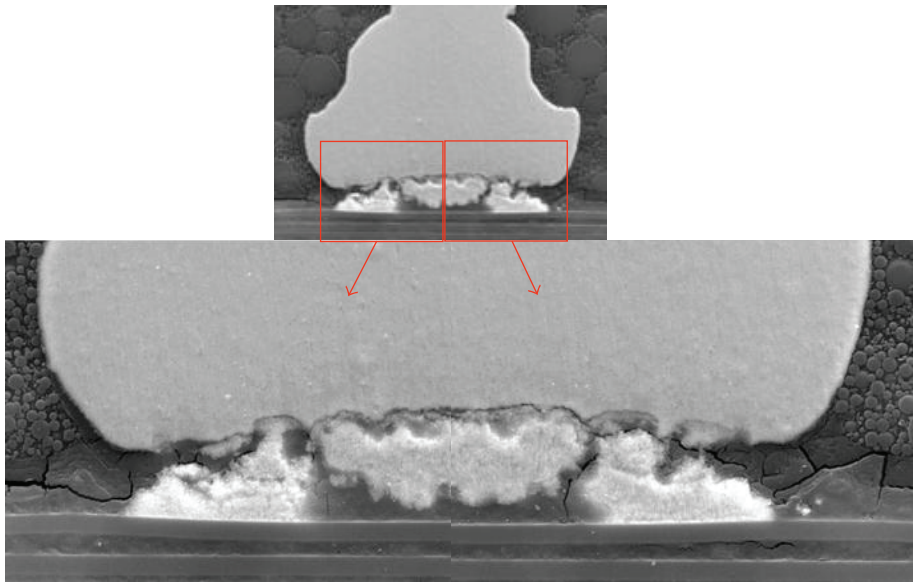

Figure 6: Typical AuAl IMC microcracks post extended UHAST stress (2000 hr).

fitted to Weibull distribution of both wire types. PdCu ball bonds shows better and larger cycles to failure compared to Au ball bonds on 110 nm device FBGA 64 package. PdCu ball bonds still exhibit longer cycle-to-failure compared to Au ball bonds in terms of thermomechanical stress, and PdCu is believed ball bond with better first ball bond integrity and able to withstand longer cold and hot cycling test with material contraction and expansion.

3.1.2. Wearout Failure Mechanisms in HAST and UHAST. The wearout failure mechanisms of CuAl interface corrosion (which induce Cu ball bond opens) are mainly due to CuAl IMC interface corrosion [1, 3–5, 12, 16, 22, 24, 26], whereas AuAl IMC interface corrosion and microcracking is widely reported by industrial and academic researchers due primarily to Kirkendall voiding [27–31]. In our study, the typical AuAl IMC interface corrosion and microcracking are indicated in Figure 5 after biased HAST 1553 hours. The whole fineline AuAl IMC microcracking occurs along the whole AuAl interface.

AuAl IMC microcracking is also observed in post UHAST-2000 hour. The failure mode is similar to post biased HAST 1553 hr for Au ball bonds on Al bondpad (as depicted in Figure 6).

Figure 7 illustrates the typical biased HAST 1817 hours CuAl IMC interface corrosion. The same failure phenomenon was observed after HAST as well as UHAST stresses, and it is most probably attributed to Cl^- attacking the edge of Cu ball bond region. Hydrolysis of IMC and $AlCl_3$ (intermediate product) under moisture environment forms aluminium(III)

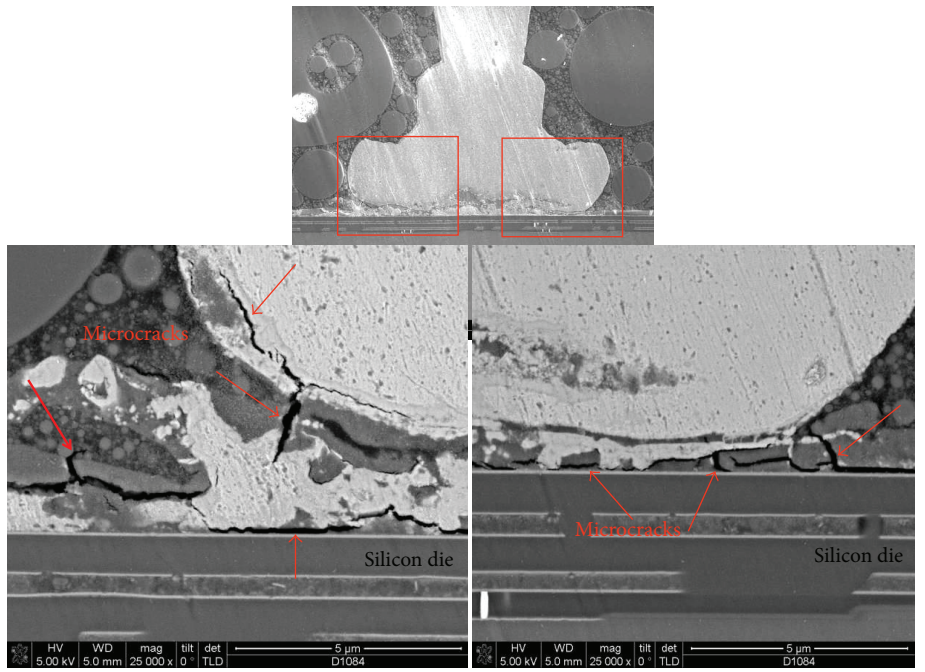

Figure 7: Typical CuAl IMC microcracks post extended HAST stress (1817 hr).

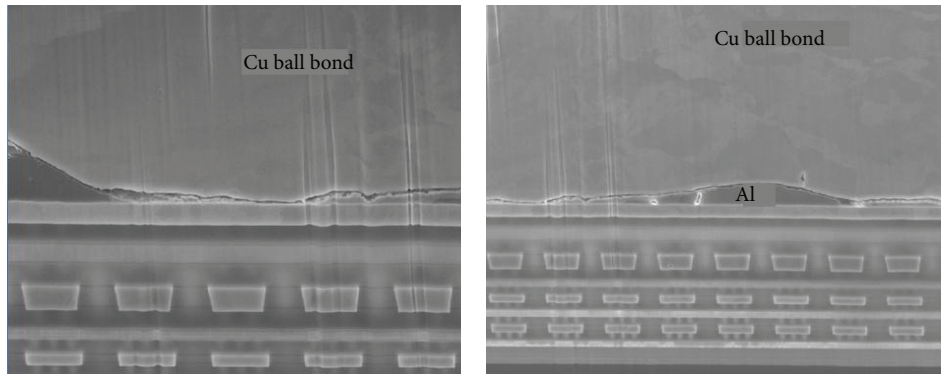

(a) (b)

Figure 8: Typical CuAl IMC microcracks post extended UHAST stress (1000 hr).

oxide which is a resistive layer, and ionic Cl^- is usually found at the corroded ball bond [1–3]. Equation (1) indicates the hydrolysis of Cu_9Al_4 into Al_2O_3 and outgassing

$$Cu_9Al_4 + 6H_2O \longrightarrow 2\left(Al_2O_3\right) + 6H_2 + 9Cu \quad \text{(out gassing which might cause IMC cracks)} \tag{1}$$

$$CuAl_2 + 3H_2O \longrightarrow Al_2O_3 + Cu + 3H_2 \quad \text{(out gassing which might cause IMC cracks)} \tag{2}$$

$$2AlCl_3 + 3H_2O \longrightarrow Al_2O_3 + 6HCl \ \text{(acidic)} \tag{3}$$

Cracking of the Al_2O_3 interface of Cu to the Cu IMC might be due to outgassing of H_2 during hydrolysis (as shown in (2) and (3)) in between Cu IMC to Cu ball bonds. Cracking usually starts at Cu ball bond periphery and will propagate towards center of Cu ball bond [1–3]. EDX analysis conducted on failed CuAl interface reveals presence of Cl, O, and Al peaks. This indicates that aluminium(III) oxide is formed a as results of corrosion reactions [3].

A representative PdCu ball bond cross-section SEM image confirms CuAl interface fineline cracking as shown in Figure 7. The fineline cracking would probably cause electrical opens in HAST stress for PdCu. The failure mechanism of Au ball bond is found similar to PdCu ball bond with similar fineline microcracking along the AuAl IMC region and caused electrical opens. Similar edge Cu ball bond microcracking is observed in post-UHAST 1000 hour opens of PdCu ball bond on Al bondpad (as shown in Figure 8).

Representative PdCu ball bond cross-section SEM image confirms CuAl interface fineline cracking as shown in Figure 9. The fineline cracking would probably cause

Table 3: Determination of IMC diffusion coefficient for each elevated temperatures.

IMC Type/(°C)	$x - x_o$	t (s) (x 1E6), 500 h	$D_1 = (x - x_0)^2/t$ (m^2s^{-1})	$x - x_o$	t (s) (x 1E6), 1000 h	$D_2 = (x - x_0)^2/t$ (m^2s^{-1})	$x - x_o$	t (s) (x 1E6), 2000 h	$D_3 = (x - x_0)^2/t$ (m^2s^{-1})	D (avg.)
CuAl/150	0.02	1.8	$2.22E-22$	0.04	1.8	$8.89E-22$	0.08	3.6	$1.78E-21$	$9.63E-22$
CuAl/175	0.06	1.8	$2.00E-21$	0.04	1.8	$8.89E-22$	0.11	3.6	$3.36E-21$	$2.08E-21$
CuAl/200	0.06	1.8	$2.00E-21$	0.04	1.8	$8.89E-22$	0.11	3.6	$3.18E-21$	$2.02E-20$
AuAl/150	0.10	1.8	$5.12E-21$	0.37	1.8	$7.69E-20$	0.76	3.6	$1.60E-19$	$8.08E-20$
AuAl/175	0.32	1.8	$5.76E-20$	0.84	1.8	$3.90E-19$	2.91	3.6	$2.35E-18$	$9.33E-19$
AuAl/200	0.63	1.8	$2.23E-19$	0.89	1.8	$4.40E-19$	3.10	3.6	$2.67E-18$	$1.11E-18$

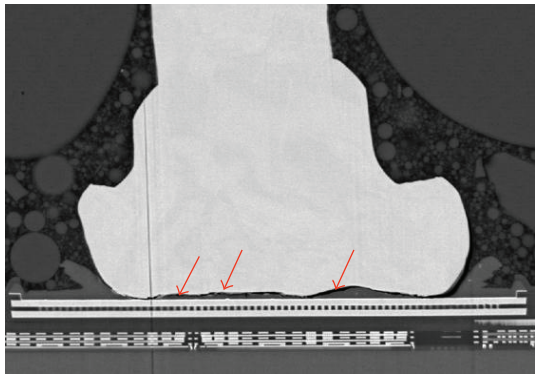

Figure 9: Typical CuAl IMC microcracks post extended TC stress (7000 cyc).

electrical opens in TC stress for PdCu. The failure mechanism of Au ball bond is found similar to PdCu ball bond with similar fineline microcracking along the AuAl IMC region and caused electrical opens. The fineline cracking after TC is due to the CTE mismatch between silicon die and Au and PdCu ball bonds under TC conditions (−40°C to 150°C) [8].

4. Diffusion Kinetics of Au and PdCu Ball Bonds

In this section, we discuss the thermal aging test that was used to accelerate the intermetallic thickness growth of CuAl and AuAl IMCs. The IMC thicknesses, diffusion coefficient (D_o) and required apparent activation energies (E_{aa}) of interdiffusion of Cu and Au atoms in Al were reported. Fick's first law of diffusion considering the concentration gradient does not change with time. It is given by (4)

$$J = D\left[\frac{C_1 - C_2}{\Delta x}\right], \tag{4}$$

where D is the diffusion coefficient (cm^2/s). The term in the square bracket is negative of the concentration gradient, dC/dx, so that the equation can be rewritten as in (5):

$$J = -D\left[\left(\frac{dC}{dx}\right)\right]. \tag{5}$$

The diffusion coefficient, D, contains the temperature dependence of the jump frequency as well as the information about the interplanar distances, which depend on crystal structure through constant D_o in (6). Graph $\ln D$ versus $(1/T)$ can be plotted by using (7)

$$D = D_o \exp\left(-\frac{E_{aa}}{RT}\right), \tag{6}$$

$$\ln D = -\left(\frac{E_{aa}}{R}\right)\left(\frac{1}{T}\right) + \ln D_o, \tag{7}$$

where self-diffusion coefficient, D_o, is a constant with unit m^2/s, E_{aa} is apparent activation energy in eV for the diffusion process, R is molar gas constant in $Jmol^{-1}K^{-1}$, and T is temperature in unit K.

Table 2 tabulates the results of E_{aa} and D_o of Au and PdCu IMCs formation of previous engineering studies [13–21] and compares them to this work. The values obtained for E_{aa} (in eV) of AuAl IMC are similar to the values investigated by Zulrich et al. [21] while E_{aa} of CuAl IMC interdiffusion is close to the value reported by Kim et al. [19, 20]. The value of D_o for CuAl IMC obtained in this study is smaller than the value of Xu et al. [13–15] while the D_o value of AuAl IMC is smaller than those previous literature values. It has been reported that intermetallic growth in AuAl and CuAl IMCs follows a parabolic law during thermal aging as in (8) [13–21]

$$x = (Dt)^{1/2}, \tag{8}$$

where x is the IMC thickness at time t and D is the diffusion coefficient. In our study, D_o value of AuAl is 1 magnitude smaller than D_o obtained for CuAl IMC. Hence, it can be concluded that the Au atom diffuse much faster than PdCu atoms in Al metallization and produce much thicker AuAl IMC layer than CuAl IMC.

Calculation of D (diffusion coefficient) can be achieved by using (9) below. The linear relationship is consistent with IMC growth being diffusion controlled, and this kinetic relationship can be described by an empirical power law,

$$x - x_o = (Dt)^{1/2}, \tag{9}$$

where x is the average thickness at annealing time t, x_o is the initial IMC thickness at $t = 0$, and D is the diffusion coefficient (in Table 3). D_1, D_2, and D_3 are the diffusion coefficients obtained after cumulative 500 hours, 1000 hours,

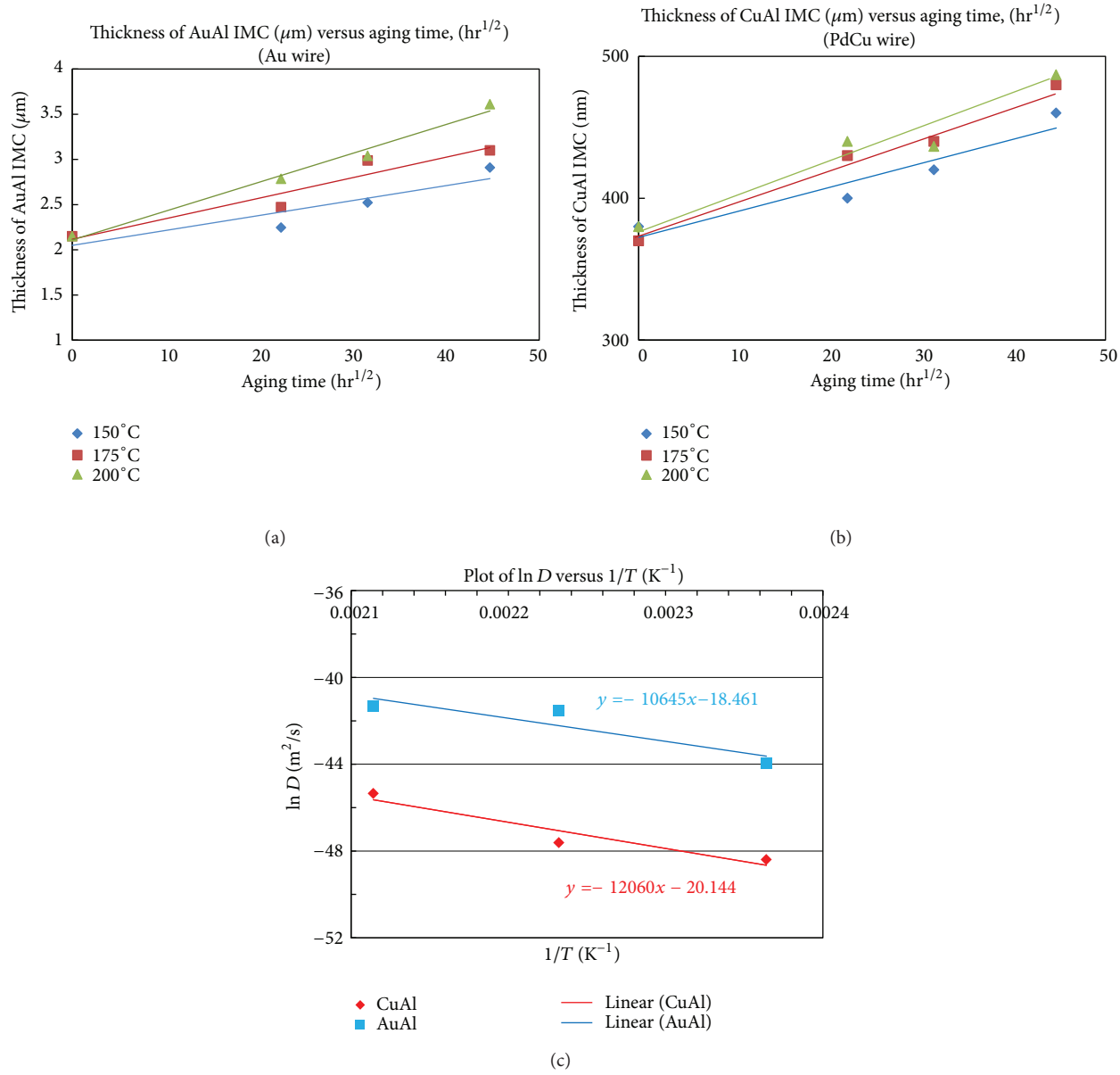

FIGURE 10: Plots of thicknesses of intermetallic compound (IMC) against aging time of Au wire (a) and PdCu wire (b) used in 110 nm device packaging (c) Plot of ln D against $1/T$ for determination of D_o values.

and 2000 hours aging, respectively. D value is calculated based on the averaged of those aging durations.

Figures 10(a) and 10(b) indicate the respective AuAl IMC and CuAl IMC thicknesses obtained in our measurement for 150°C, 175°C, and 200°C aging temperatures. It clearly indicates that Au atoms diffuse at least 5 times faster than PdCu atoms in Al metallisation of 110 nm device.

The respective D_o (diffusion coefficient) of AuAl IMC and CuAl IMCs can be determined by plotting ln D against $1/T$ after high temperature storage life tests at 3 temperatures (150°C, 175°C, and 200°C). Figure 10(c) reveals the extrapolation of D_o for the AuAl and CuAl IMCs. AuAl IMC is reported with faster interdiffusion rate if compared to CuAl IMC in 110 nm device. The value of D_o can be determined from the intercept of the plot of ln D against $1/kT$ (as shown in Figure 10(c)).

5. Postextended Reliability Stresses Ball Bond Shear and Wire Pull Strength Analysis (Au versus PdCu Ball Bonds)

Mechanical strengths (ball bond shear and wire pull strength) of PdCu and Au ball bonds were analyzed at extended hours and cycles of reliability stresses. The main objective is to confirm if the ball bonds are robust even after the extended reliability stress testing. The typical minimum shear strength (in g) and minimum wire pull strength (in gf) of 0.80 mil wire diameter are 14 g and 2.5 gf, respectively. The mean values

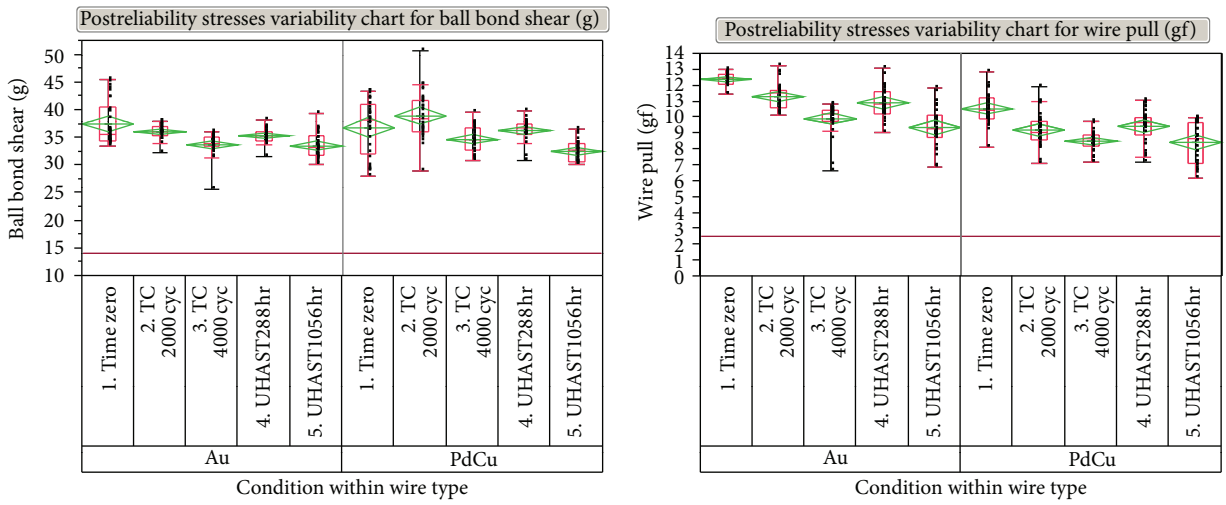

FIGURE 11: Box plots of ball bond shear (a) and wire pull strength and of (b) post reliability stresses for Au and PdCu wires in 110 nm device packaging.

of ball bond shear and wire pull strength are analyzed and compared to time zero before stress testing.

It is observed that the ball shear strength degraded gradually over time. However, they far exceed the minimum shear value of 14 g (as shown in Figure 11(a)). Figure 11(b) indicates similar degradation trend for wire pull strength when comparing Au and PdCu ball bonds. PdCu ball bonds exhibit faster degradation trend compared to Au ball bonds.

6. Conclusion

In Au and PdCu wire bonding evaluations on 110 nm devices, we have successfully characterized the wearout reliability margins for HAST and UHAST and determined the diffusion kinetics of both wire types used in nanoscale semiconductor packaging.

The technical findings are summarized as the following.

(1) PdCu ball bond exhibits a higher time to failure (Weibull fitted distribution) compared to Au ball bonds in HAST wearout reliability plots. PdCu ball bonds showed a slightly lower UHAST wearout hour to failure but still far exceeding the JEDEC standard of minimum 96-hour surviving hours rate.

(2) Wearout failure mechanism of HAST and UHAST stress testing belong to CuAl and AuAl IMCs interface corrosion and microcracking which induced electrical ball bond opens.

(3) The values obtained for E_{aa} (in eV) of AuAl IMC formation (1.04 eV) is similar to the values investigated by Zulrich et al. [21], while E_{aa} of CuAl IMC interdiffusion (1.18 eV) is close to the value reported by Kim et al. [19, 20]. The value of D_o for CuAl IMC obtained in this study is smaller than the value of Xu et al. [13–15], while D_o of AuAl IMC is a bit smaller than those previous literature values. In our study, D_o value of AuAl is 1 magnitude smaller than D_o obtained for CuAl IMC. Hence, it can be concluded that the Au atom diffuse much faster than PdCu atoms in Al metallization [8, 16, 21, 27].

(4) It clearly indicates that Au atoms diffuse at least 5 times faster than PdCu atoms in Al metallization of the 110 nm flash device tested. This could be easily estimated from the comparison of IMC thickness developed over time comparing CuAl and AuAl IMCs.

(5) Ball shear strength degraded gradually over time for both PdCu and Au ball bonds. However, it is still far exceeding the minimum shear value of 14 g and wire pull value of 2.5 gf. A similar degradation trend for wire pull strength comparing Au and PdCu ball bonds was also observed. Additionally, PdCu ball bonds exhibit faster degradation trend compare to Au ball bonds.

Acknowledgment

The authors would like to take this opportunity to thank Spansion management (Gene Daszko, Tony Reyes, and Chong Hin Lian) for their management support for this study.

References

[1] C. L. Gan, T. T. Toong, C. O. Lim, and C. Y. Ng, "Environmental friendly package development by using copper wirebonding," in *Proceedings of the 34th International Electronics Manufacturing Technology Conference (IEMT '10)*, Malacca, Malaysia, December 2010.

[2] C. L. Gan, E. K. Ng, B. L. Chan, and U. Hashim, "Reliability challenges of Cu wire deployment in flash memory packaging,"

in *Proceedings of IEEE CPMT IMPACT*, pp. 498–501, Taipei, Taiwan, 2012.

[3] C. L. Gan, E. K. Ng, B. L. Chan, U. Hashim, and F. C. Classe, "Technical barriers and development of Cu wirebonding in nanoelectronic device packaging," *Journal of Nanomaterials*, vol. 2012, Article ID 173025, 7 pages, 2012.

[4] C. W. Tan, A. R. Daud, and M. A. Yarmo, "Corrosion study at Cu-Al interface in microelectronics packaging," *Applied Surface Science*, vol. 191, no. 1–4, pp. 67–73, 2002.

[5] T. Uno, "Bond reliability under humid environment for coated copper wire and bare copper wire," *Microelectronics Reliability*, vol. 51, no. 1, pp. 148–156, 2011.

[6] Z. W. Zhong, "Overview of wire bonding using copper wire or insulated wire," *Microelectronics Reliability*, vol. 51, no. 1, pp. 4–12, 2011.

[7] J. Chen, D. Degryse, P. Ratchev, and I. De Wolf, "Mechanical issues of Cu-to-Cu wire bonding," *IEEE Transactions on Components and Packaging Technologies*, vol. 27, no. 3, pp. 539–545, 2004.

[8] G. G. Harman, *Wirebonding in Microelectronic: Materials, Processes, Reliability, and Yield*, McGraw Hill, New Year, NY, USA, 2nd edition, 1999.

[9] C. J. Hang, C. Q. Wang, M. Mayer, Y. H. Tian, Y. Zhou, and H. H. Wang, "Growth behavior of Cu/Al intermetallic compounds and cracks in copper ball bonds during isothermal aging," *Microelectronics Reliability*, vol. 48, no. 3, pp. 416–424, 2008.

[10] JEDEC Standard JESD 47, "Stress test driven qualification of integrated circuits," 2012.

[11] J. W. McPherson, *Reliability Physics and Engineering: Time to Failure Modeling*, Springer, 1st edition, 2010.

[12] C. L. Gan, E. K. Ng, B. L. Chan, T. Kwuanjai, and U. Hashim, "Wearout reliability study of Cu and Au wires used in flash memory fine line BGA package," in *Proceedings of IEEE CPMT IMPACT*, pp. 494–497, 2012.

[13] H. Xu, C. Liu, V. V. Silberschmidt, and Z. Chen, "Growth of intermetallic compounds in thermosonic copper wire bonding on aluminum metallization," *Journal of Electronic Materials*, vol. 39, no. 1, pp. 124–131, 2010.

[14] H. Xu, C. Liu, V. V. Silberschmidt, S. S. Pramana, T. J. White, and Z. Chen, "A re-examination of the mechanism of thermosonic copper ball bonding on aluminium metallization pads," *Scripta Materialia*, vol. 61, no. 2, pp. 165–168, 2009.

[15] H. Xu, C. Liu, V. V. Silberschmidt et al., "Behavior of aluminum oxide, intermetallics and voids in Cu-Al wire bonds," *Acta Materialia*, vol. 59, no. 14, pp. 5661–5673, 2011.

[16] C. W. Tan and A. R. Daud, "The effects of aged Cu-Al intermetallics to electrical resistance in microelectronics packaging," *Microelectronics International*, vol. 19, no. 2, pp. 38–43, 2002.

[17] J. P. Shaffer, A. Saxena, S. D. Antolovich, T. H. Sanders, and S. B. Warner, *The Science and Design of Engineering Materials*, Richard D. Irwin, Chicago, Ill, USA, 1995.

[18] R. Pelzer, M. Nelhiebel, R. Zink, S. Wohlert, A. Lassnig, and G. Khatibi, "High temperature storage reliability investigation of the Al-Cu wirebond interface," *Microelectronics Reliability*, vol. 52, no. 9-10, pp. 1966–1970, 2012.

[19] H. J. Kim, J. Y. Lee, K. W. Paik et al., "Effects of Cu/Al intermetallic compound (IMC) on copper wire and aluminum pad bondability," *IEEE Transactions on Components and Packaging Technologies*, vol. 26, no. 2, pp. 367–374, 2003.

[20] H. J. Kim, J. Y. Lee, K. W. Paik et al., "Effects of Cu/Al intermetallic compound (IMC) on copper wire and aluminum pad bondability," in *Proceedings of IEEE International Symposium on Electronic Materials and Packaging*, pp. 44–51, 2001.

[21] C. M. Zulrich, A. Hashibon, J. Svoboda, C. Elsasser, D. Helm, and H. Riedel, "Diffusion Kinetics in aluminium-gold bond contacts from first principles density functional calculations," *Acta Materialia*, vol. 59, pp. 7634–7644, 2011.

[22] F. C. Classe and S. Gaddamraja, "Long term isothermal reliability of copper wire bonded to thin 6.5 μm aluminum," in *Proceedings of the 34th International Reliability Physics Symposium (IRPS '11)*, pp. 685–689, 2011.

[23] "Accelerated moisture resistance- Unbiased HAST Test," JEDEC Specification *JESD22A-118A*, 2011.

[24] C. F. Yu, C. M. Chan, L. C. Chan, and K. C. Hsieh, "Cu wire bond microstructure analysis and failure mechanism," *Microelectronics Reliability*, vol. 51, no. 1, pp. 119–124, 2011.

[25] S. Murali, N. Srikanth, Y. M. Wong, and C. J. Vath, "Fundamentals of thermo-sonic copper wire bonding in microelectronics packaging," *Journal of Materials Science*, vol. 42, no. 2, pp. 615–623, 2007.

[26] S. H. Kim, J. W. Park, S. J. Hong, and J. T. Moon, "The interface behavior of the Cu-Al bond system in high humidity conditions," in *Proceedings of 60th IEEE CPMT ECTC*, pp. 545–549, 2010.

[27] M. N. Zulkifli, S. Abdullah, N. K. Othman, and A. Jalar, "Some thoughts on bondability and strength of gold wire bonding," *Gold Bulletin*, vol. 8, 2012.

[28] C. D. Breach and F. Wulff, "New observations on intermetallic compound formation in gold ball bonds: general growth patterns and identification of two forms of Au_4Al," *Microelectronics Reliability*, vol. 44, no. 6, pp. 973–981, 2004.

[29] C. D. Breach and F. Wulff, "Oxidation of Au4Al in un-moulded gold ballbonds after high temperature storage (HTS) in air at 175 ∘C," *Microelectronics Reliability*, vol. 46, no. 12, pp. 2112–2121, 2006.

[30] A. Karpel, G. Gur, Z. Atzmon, and W. D. Kaplan, "Microstructural evolution of gold-aluminum wire-bonds," *Journal of Materials Science*, vol. 42, no. 7, pp. 2347–2357, 2007.

[31] M. K. Md Arshad, I. Ahmad, A. Jalar, G. Omar, and U. Hashim, "The effects of multiple zincation process on aluminum bond pad surface for electroless nickel immersion gold deposition," *Journal of Electronic Packaging*, vol. 128, no. 3, pp. 246–250, 2006.